VNU Journal of Science: Mathematics – Physics, Vol. 35, No. 3 (2019) 85-93

VNU Journal of Science: Mathematics - Physics

Journal homepage: https://js.vnu.edu.vn/MaP

Original Article

Electrochemical Performance of Fe_2O_3/AB-Based Composite Electrode

Trinh Tuan Anh, Bui Thi Hang*

International Training Institute for Materials Science (ITIMS), Hanoi University of Science and Technology (HUST), Hanoi, Vietnam

Received 04 May 2019
Revised 29 May 2019; Accepted 01 June 2019

Abstract: In this study, Fe_2O_3 nanoparticles (nm) and microparticles (µm) were used as active materials and Acetylene Black carbon (AB) as an additive to prepare Fe_2O_3/AB composites to find a suitable material for Fe-air battery anode. The effects of grain size of iron oxide particles and additives on the electrochemical behavior of Fe_2O_3/AB composite electrodes in alkaline solution were investigated using cyclic voltammetry (CV), galvanostatic cycling and electrochemical impedance spectroscopy (EIS) measurements. The study results show that iron oxide nanoparticles provided better cyclability than iron oxide microparticles. The impedance of electrode increased during cycling, but the nm-Fe_2O_3/AB electrode gave smaller resistance than the µm-Fe_2O_3/AB one. The additives showed strong effects on the electrochemical behaviors of iron oxide electrodes. The AB additive enhanced the electric conductivity of Fe_2O_3/AB electrode and thus increased the redox reaction rate of iron oxide while K_2S interacted with and broke down the passive layer leading to improved cyclability and giving higher capacity for Fe_2O_3/AB electrodes.

Keywords: Fe_2O_3 nanoparticles, Fe_2O_3 microparticles, K_2S additive, Fe_2O_3/AB composite electrode, Fe-air battery anode

1. Introduction

High energy density for metal/air batteries has been the focus of attention in recent years for applications involving electric vehicles [1-3]. Iron is a potential candidate for metal/air battery anode and is also used in nickel/iron battery because of high theoretical energy (0.96 Ah/g) and low cost [4-

*Corresponding author.
Email address: hang@itims.edu.vn

https//doi.org/ 10.25073/2588-1124/vnumap.4348

7,8]. However, the problem of iron electrode is the passive layer of $Fe(OH)_2$ formed during cycling leading to a low utilization coefficient. Further, the potential of the $Fe/Fe(OH)_2$ couple is only slightly more negative than that of the hydrogen evolution potential in alkaline solution [5,7] thereby there is a simultaneous evolution of hydrogen during charging [8-9]. This is the cause of the low charge/discharge efficiency and high self-discharge rate of iron electrode. To overcome the limitations of the iron electrode, a number of additives are incorporated in the iron electrode during fabrication [6, 8-11] or in electrolyte [6, 10-14] or both [6, 10-11, 14]. To increase the active material surface area, in the present study, we prepared Fe_2O_3/C using Acetylene Black carbon (AB) and iron oxide for use as anode in Fe/air battery. In addition, K_2S is used as an additive to electrolyte to improve the limitations of the iron electrode.

2. Experimental

Fe_2O_3 nanopartilces (nm-Fe_2O_3) and microparticles (μm-Fe_2O_3)(Wako Pure Chemical Co.) and acetylene black (AB, Denki Kagaku Co. Ltd.) were used as the iron sources and carbon additives to prepare the Fe_2O_3/AB materials by mixing of 50 : 50 wt% Fe_2O_3 and AB followed by ball milling. The Fe_2O_3/ABcomposite electrodes were fabricated by mixing 90 wt% Fe_2O_3/ABmaterialsobtained after ball milling with 10wt%polytetrafluoroethylene (PTFE, Daikin Co.)binder followed by rolling and punching into the form of a pellet with 1 cm in diameter. Thus, in Fe_2O_3/AB composite electrodes, Fe_2O_3, AB and binder components are 45, 45 and 10 wt%, respectively.

To investigate the effect of Fe_2O_3 particle size as well as the K_2S additive on the electrochemical properties of the Fe_2O_3/AB electrodes, cyclic voltammetry (CV) studies have been carried out in three-electrode glass cells with Fe_2O_3/AB composite electrode as the working electrode, Pt mesh as the counter electrode and Hg/HgO as the reference electrode. The electrolyte was 8 $moldm^{-3}$ KOH aqueous solution or 7.99 $moldm^{-3}$ KOH + 0.01 $moldm^{-3}$ K_2S aqueous solution. CV measurements were taken at a scan rate of 2 mV s^{-1} and within a voltage range of −1.3 V to −0.1 V. Charge/discharge measurements were conducted on three-electrode glass cells. In the charge course, the current density of 50 mA cm^{-2} was used with a cutoff potential of −1.2 V whereas in the discharge course, a constant current density of 2.0 mA cm^{-2} was applied with a cutoff potential of −0.1 V. The electrochemical impedance spectroscopy (EIS) studies have been performed on a three-electrode glass cell assembly using Auto Lab system. The impedance spectra were recorded after the cell was cycled and stopped at open circuit potential (OCP) followed by a rest period of 1 hour. The AC perturbation signal has been fixed at 10 mV, and the frequency range was from 10^{-2} to 10^5 Hz in the EIS. In all electrochemical measurements, we used fresh electrodes without pre-cycling.

3. Results and discussion

Nanoparticles (nm) and microparticles (μm) of Fe_2O_3 have been used as electrode active materials to investigate the effect of Fe_2O_3 particle size on their electrochemical properties. The SEM images of nm- Fe_2O_3 and μm-Fe_2O_3 samples are shown in Figs. 1a and 1b, respectively. The nm-Fe_2O_3 particles are less than 100 nm and relatively uniform. They look like little balls. Unlike the nm- Fe_2O_3 sample, the SEM image of the μm-Fe_2O_3 in Fig. 1b shows mixed particle size and shape. They consist of Fe_2O_3 flat flakes with dimensions ranging from several hundred nanometers to several ten micrometers. Different sizes and shapes of the nm-Fe_2O_3 and μm-Fe_2O_3 samples shall affect the electrochemical characterization of the Fe_2O_3 electrode.

3.1. Effect of particle size and shape of iron oxide and additive on the electrochemical behavior of Fe_2O_3/AB composite electrode

The cyclic voltammetry (CV) measurements of the nm-Fe_2O_3/AB composite electrode (Fe_2O_3: AB: PTFE = 45:45: 10 wt%) are presented in Fig. 2a. On the oxidation scan from −1.3 V to −0.1 V, two oxidation peaks of Fe/Fe(II)(a_1), Fe(II)/Fe(III)(a_2) occur at about −0.9 V and −0.4 V, whereas on the reverse direction, only one reduction peak corresponding to Fe (III)/Fe(II)(c_1) occurs at about −1.0 V along with the hydrogen evolution peak. The reduction peak of Fe(II)/Fe(c_2) is completely masked by hydrogen evolution. Particularly, the oxidation peak a_2 is very large and broad compared to the a_1 peak. This may be due to the formation of $Fe(OH)_2$ which inhibits the oxidation of the inner layer of the iron leading to increase the overpotential of Fe/Fe(II) reaction. Consequently, a_2 peak includes oxidation reactions of both Fe/Fe(II) and Fe(II)/Fe(III). This is the reason why a_2 is a very large peak compared to a_1 peak. The redox peak currents increases during initial cycles and then decrease upon further cycling. In the first discharge, $Fe(OH)_2$ was formed on the surface of iron and carbon via an intermediate soluble species, $HFeO_2^-$. The passive layer $Fe(OH)_2$ inhibited the oxidation of inner iron and thus overpotential increased. In initial cycles, $Fe(OH)_2$ layer was thin, the oxidation reaction rate was high. Further cycling, insulated $Fe(OH)_2$layer became thicker resulting in larger electrode resistance and consequently redox current decreased.

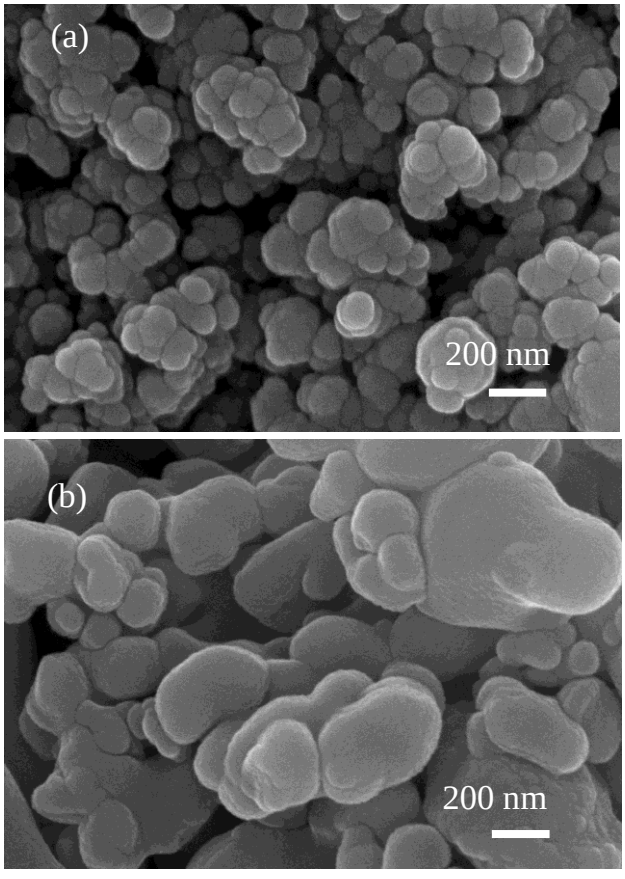

Figure 1. SEM images of (a) nm-Fe_2O_3 and (b) µm-Fe_2O_3 samples.

In order to investigate the effect of grain size and morphology of Fe_2O_3 on the electrochemical behaviors of Fe_2O_3/AB electrodes, CV measurements were carried out on the μm-Fe_2O_3/AB electrode (Fe_2O_3: AB: PTFE = 45:45: 10 wt%) and the results are presented in Fig. 3a.Similar to nm-Fe_2O_3/AB, the redox peaks a_1, a_2, c_1 also appear at around − 0.9, − 0.5 and −0.95 V respectively, and c_2 peak is masked by hydrogen peak. However, the current intensity of these peaks decreases with increasing cycle number.

Compared to nm-Fe_2O_3/AB sample (Fig. 2a), the redox peaks of μm-Fe_2O_3/AB (Fig. 3a) electrode are very small. This proves that the size and shape of Fe_2O_3 particles strongly influence their electrochemical properties. In this case, nm-Fe_2O_3 particles exhibit better cyclability than μm-Fe_2O_3. This could be explained in view of the Fe_2O_3 nanoparticles having a larger surface area than the Fe_2O_3 microparticles, so that the redox reaction rate of nm- Fe_2O_3 is greater than μm-Fe_2O_3 and therefore it has better cyclability.

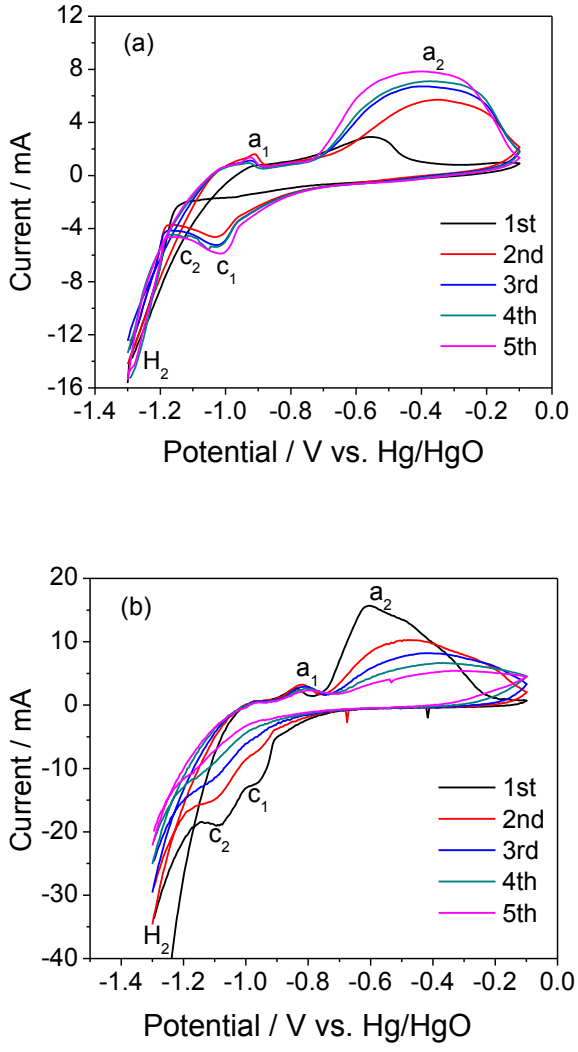

Figure 2.CV profiles of nm-Fe_2O_3 /AB composite electrodes(Fe_2O_3:AB:PTFE = 45:45:10 wt.%) in (a) KOH and (b) KOH+K_2S electrolyte solution.

The role of adding K_2S in the electrolyte on the cyclability of the nm-Fe_2O_3/AB and µm-Fe_2O_3/AB electrodes have been investigated and the results are presented in Fig. 2b and 3b respectively. Comparing the CV results of the nm-Fe_2O_3/AB sample in KOH solution (Fig. 2a) with those in KOH+K_2S solution (Fig. 2b), it can be seen that adding K_2S to the electrolyte solution (2b), beside the appearance a_1, a_2 and c_1 peaks, the reduction peak of Fe (II)/Fe(c_2) is observable and it is separated from the hydrogen evolution peak. This demonstrates that the amount of hydrogen evolution is partially suppressed and the reaction rate of Fe/Fe(II) couple is increased while its over-potential is decreased with the presence of K_2S in the electrolyte solution. In other words, the reaction rate of Fe/Fe(II) is increased and its overpotential is decreased by sulfide ion. There may be an effect of the adsorbed sulfide ion, which interacts strongly with Fe(I), Fe(II) or Fe(III) in the oxide film and promotes the dissolution of iron and enhance the bulk conductivity of the electrode, thereby improving cycleability [15-16].

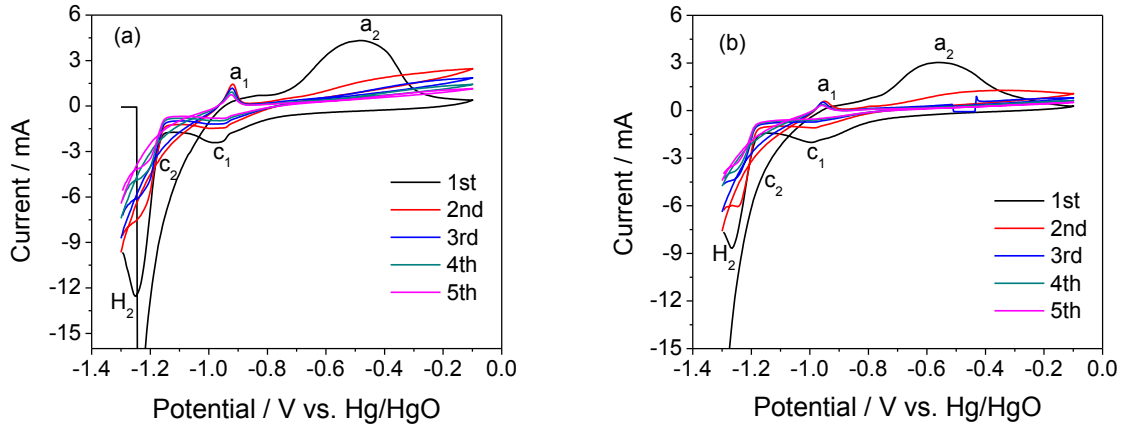

Figure 3.CV profiles of µm-Fe_2O_3 /AB composite electrodes(Fe_2O_3:AB:PTFE = 45:45:10 wt.%) in (a) KOH and (b) KOH+K_2S electrolyte solution.

Further cycling, the current under these peaks decreased and deposition peak of iron c_2 is gradually masked by hydrogen. This suggests that the inner resistance of the electrode was increased due to the insulating of $Fe(OH)_2$ layer forming during the oxidation. When K_2S is present in the electrolyte solution, initially the reaction rates of the Fe/Fe(II) and Fe(II)/Fe (III) couples are increased, but on subsequent sweeping, the formed $Fe(OH)_2$ film is thicker, the passivation overwhelms the increase in the redox reaction rate supported by K_2S thereby reducing the redox current. Consequently, K_2S additive proved the positive effects on the electrochemical behaviors of nm-Fe_2O_3/AB composite electrode.

The CV results of µm-Fe_2O_3/AB electrode in electrolyte containing S^{-2} are depicted in Fig. 3b. In comparison to CV results in KOH electrolyte (Fig.3a), the CV profiles in both cases are relatively similar. When K_2S is introduced into the electrolyte solution (Fig. 3b), the a_1, a_2, and c_1 peaks still appear at the same potentials as in Figure 3a. As the number of sweeps increases, the current intensity in both couple peaks decreases. No significant differences are observed in the CV profiles of the µm-Fe_2O_3/AB electrodes in KOH and KOH+ K_2S. Thus, for the µm-Fe_2O_3/AB composite sample, the presence of K_2S in the electrolyte does not have a positive effect on the electrochemical behavior of µm-Fe_2O_3 as well as the cyclability of the µm-Fe_2O_3/AB electrode.

3.2. Electrochemical Impedance spectroscopy (EIS) of nm-Fe_2O_3/AB and µm-Fe_2O_3/AB composite electrodes in electrolyte with and without additive

Electrode resistance was determined for nm-Fe_2O_3/AB và µm-Fe_2O_3/AB composite electrodes in KOH and KOH+K_2S electrolytes using electrochemical impedance spectroscopy (EIS). The EIS measurements were carried out before and after five initial cycles at open circuit potential (OCP) and the results are shown in Figs. 4 and 5 respectively. Before and after cycling, each spectrum consists of a semicircle in a high frequency region, which was assigned to the interfacial response, followed by a straight line in the lower frequency region corresponding to Warburg impedance. As the limitation of the apparatus was 100 Hz, straight line at lower frequencies is either short or not present.

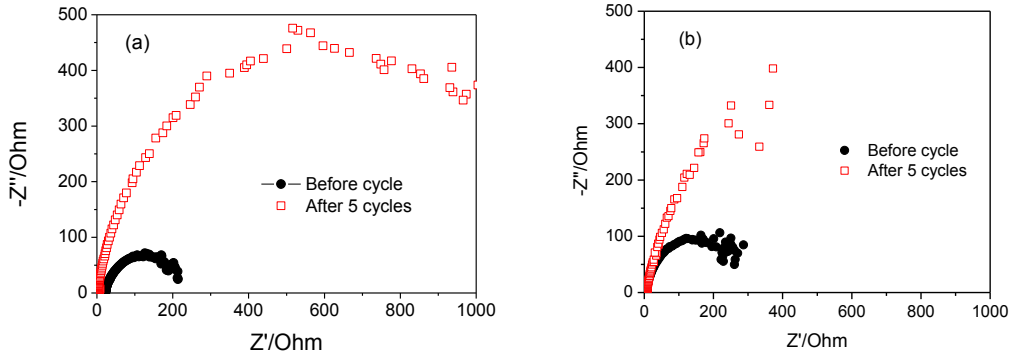

Figure 4. Electrochemical impedance spectroscopy (EIS) of nm-Fe_2O_3/AB electrode (Fe_2O_3:AB:PTFE = 45:45:10 wt.%) in (a) KOH and (b) KOH + K_2S electrolyte solution

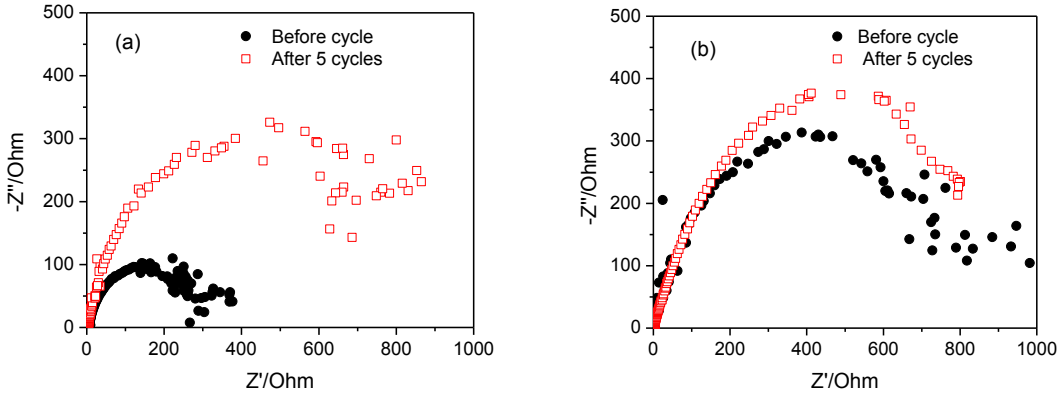

Figure 5. Electrochemical impedance spectroscopy (EIS) of µm-Fe_2O_3/AB electrode (Fe_2O_3:AB:PTFE = 45:45:10 wt.%) in (a) KOH and (b) KOH + K_2S electrolyte solution.

In the case of KOH electrolyte (Figs. 4a and 5a), before cycling, the semicircle was observed with a straight line in the lower frequency region. After cycling, the semicircle was observable but not completely and semicircle diameter of the electrode after cycling is larger than that before cycle. This suggested that the resistance of electrodes increased after cycling and gradually increased with increase in cycle number. The semicircle diameter of nm-Fe_2O_3/AB electrode is a little smaller than that of µm-Fe_2O_3/AB electrode in KOH suggests that nm-Fe_2O_3/AB electrode has lower resistance than µm-Fe_2O_3/AB. These results are consistent with the CV results (Figs.2 and 3), as the redox

current decreased with repeated cycling and nm-Fe_2O_3/AB electrodes have better cyclability than µm-Fe_2O_3/AB. This is reasonable since resistance of electrode gradually increased with repeated cycling and µm-Fe_2O_3/AB electrodes give larger resistance than nm-Fe_2O_3/AB electrode.

In the case of electrolyte solution containing K_2S additive (Fig. 4b and 5b), the semicircle diameters of the electrodes after cycling are also larger than those of the electrodes before cycle similar to that observed in KOH solution thereby implying that the electrode resistance also increases during cycling in additive electrolyte. Remarably, the semicircle diameters of electrodes before and after cycling in the electrolyte containing K_2S (Figs. 4b and 5b) are larger than those in the base electrolyte (Figs. 4a and 5a). These results demonstrate that the resistance of the Fe_2O_3/AB electrode in the additive electrolyte is larger than that in the free additive electrolyte and can be ascribed to the S^{2-} ion in the electrolyte solution adsorbed on the surface of the Fe_2O_3/AB electrode causing an increase in the contact resistance between the electrode surface and the electrolyte solution. However the semicircle diameter of nm-Fe_2O_3/AB electrode before cycle is a little smaller than that after cycle while it is much smaller than that of µm-Fe_2O_3/AB electrode after cycle. This tendency is consistent with the of CV profiles (Figs. 2b and 3b). In the case of nm-Fe_2O_3/AB electrode (Fig. 2b), the presence of the K_2S additive in the electrolyte enhances the redox reaction rate of the Fe_2O_3/AB electrode. Therefore, the presence of S^{2-} in the electrolyte solution on the one hand increases the resistance of the Fe_2O_3/AB electrode, but on the other hand it also enhances the redox reaction rate of the electrode. However, the current intensity still decreased with increase in cycle number due to the passive layer $Fe(OH)_2$ formed during the discharge. Adding K_2S into the electrolyte solution, initially the reaction rate of the Fe/Fe(II) and Fe(II)/Fe(III) couples increases, but the $Fe(OH)_2$ layer becomes thicker upon repeated cycling, passivation dominates the increase in the reaction rate leading to reducing redox current. In the case of µm-Fe_2O_3/AB electrode, the presence of the K_2S additive in electrolyte did not provide any positive effect either in term of cyclability of iron (Fig. 3b) nor the impedance of electrode before and after cycling is too large (Fig. 5b) than that of nm-Fe_2O_3/AB electrode. Consequently, under these experimental conditions, nm-Fe_2O_3/AB electrode provided better cyclability, higher redox reaction rate than µm-Fe_2O_3/AB electrode.

3.3. Cycle performance of nm-Fe_2O_3/AB electrode

To obtaine the cycle performance of nm-Fe_2O_3/AB electrode, the galvanostatic cycle measurement in KOH + K_2S solution was carried out, the results are presented in Figs. 6 and 7.

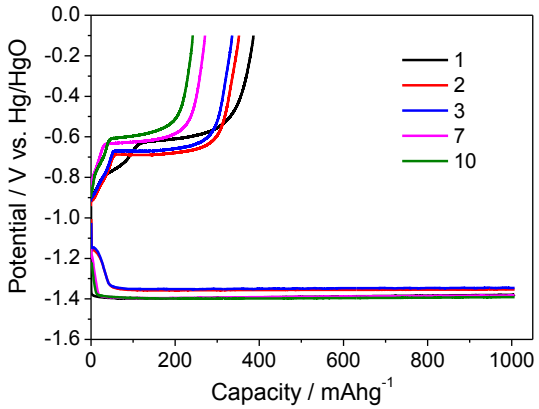

Figure 6. Charge-discharge curves of nm-Fe_2O_3/AB electrode in KOH + K_2S solution

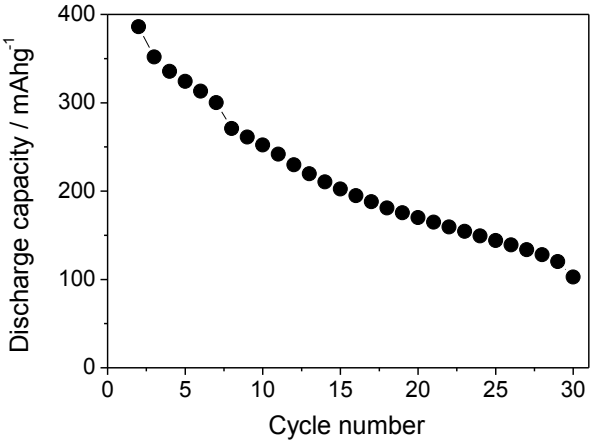

Figure 7. Discharge capacity of nm-Fe_2O_3/AB electrode in KOH + K_2S solution.

One oxidation plateau was observed at about –0.65 V in the discharge curves (Fig.6) correspondence to the oxidation reactions of Fe/Fe(II) and Fe(II)/Fe(III). The plateau was shortened when repeated cycling. These results suggest that the discharge capacity decreased with further cycling. The changing of discharge capacity of nm-Fe_2O_3/AB electrode was consistent with that of CV profiles (Fig. 2b).

Fig. 7 show the cycle performance of the nm-Fe_2O_3/AB electrode in KOH+K_2S solution. High discharge capacity attained at the initial cycle and then gradually decreased with further cycling. These results demonstrate the capacity retention was low at this cycling condition. To meet the actual application requirements the capacity retention still need further improvements.

4. Conclusion

The size and morphology of iron oxide strongly affected the electrochemical properties of Fe_2O_3/AB composite electrodes. Fe_2O_3 nanoparticles provided higher redox reaction rate and better cyclability than Fe_2O_3 microparticles. Besides that, nm-Fe_2O_3/AB composite electrodes gave smaller resistance than μm-Fe_2O_3/AB composite electrodes.

The nm-Fe_2O_3/AB composite electrodes in electrolyte containing K_2S additive showed the improved redox reaction rate of Fe/Fe(II) and Fe(II)/Fe(III) couples and significantly suppressed hydrogen evolution during cycling whereas μm-Fe_2O_3/AB composite electrodes did not show such behaviors. It revealed that K_2S has positive effects on the electrochemical properties of nm-Fe_2O_3/AB composite electrodes but negligibly affect on the μm-Fe_2O_3/AB one.

The resistance of the Fe_2O_3/AB composite electrodes after cycling is higher than that of before cycling in both electrolytes containing K_2S additive and free additive. The electrochemical impedance of the Fe_2O_3/AB electrodes in the electrolyte containing K_2S additive increased with respect to that in the basic KOH electrolyte. The nm-Fe_2O_3/AB composite electrode in electrolyte containing K_2S additive gave high discharge capacity at initial cycle and then gradually decreased with further cycling.

Acknowledgements

This research is funded by Vietnam National Foundation for Science and Technology Development (NAFOSTED) under grant number 103.02-2018.04.

References

[1] L. Ojefors, L. Carlsson, An iron - air vehicle battery, J. Power Sources 2 (1977-1978) 287-296.

[2] K.F. Blurtin, A.F. Sammells, Metal/air batteries: Their status and potential - a review, J. Power Sources 4 (1979) 263-279.

[3] A.M. Kannan, A.K. Shukla, Rechargeable Iron/Air cells employing bifunctional oxygen electrodes of oxide pyrochlores, J. Power Sources 35 (1991) 113-121.

[4] K. Vijayamohanan, T.S. Balasubramanian, A.K. Shukla, Rechargeable alkaline iron electrodes, J. Power Sources 34 (1991) 269-285.

[5] C. Chakkaravarthy, P. Periasamy, S. Jegannathan, K.I. Vasu, The nickel/iron battery, J. Power Sources 35 (1991) 21-35.

[6] M. Jayalakshmi, B.N. Begumi, V.R. Chidambaram, R. Sabapathi, V.S. Muralidharan, Role of activation on the performance of the iron negative electrode in nickel/iron cells, J. Power Sources 39 (1992) 113-119.

[7] A.K. Shukla, M.K. Ravikumar, T.S. Balasubramanian, Nickel-Iron Storage Batteries,J. Power Sources51 (1994) 29-36.

[8] C.A. Caldas, M.C. Lopes. I.A. Carlos, The role of FeS and $(NH_4)_2CO_3$ additives on the pressed type Fe electrode, J. Power Sources 74 (1998) 108-112.

[9] C.A.C. Souza, I.A. Carlos, M.C. Lopes, G.A. Finazzi, M.R.H. de Almeida., Self-discharge of Fe-Ni alkaline batteries, J. Power Sources132 (2004) 288-290.

[10] G.P. Kalaignan, V.S. Muralidharan, K.I. Vasu, Triangular potential sweep voltammetric study of porous iron electrodes in alkali solutions, J. Appl. Electrochem. 17 (1987) 1083-1092.

[11] K. Micka, Z. Zabransky, Study of iron oxide electrodes in an alkaline electrolyte, J. Power Sources 19 (1987) 315-323.

[12] J. Cerny, Voltammetric study of an iron electrode in alkaline electrolytes, J. Power Sources 25 (1989) 111-122.

[13] P. Periasamy, B.R. Babu, S.V. Iyer, Cyclic voltammetric studies of porous iron electrodes in alkaline solutions used for alkaline batteries, J. Power Sources 58 (1996) 35-40.

[14] Bui Thi Hang, Tomonori Watanabe, Minato Egashira, Izumi Watanabe, Shigeto Okada, Jun-ichi Yamaki, The effect of additives on the electrochemical properties of Fe/C composite for Fe/air battery anode, J. Power Sources 155 (2006) 461-469.

[15] D.W. Shoesmith, P. Taylor, M.G. Bailey, B. Ikeda, Electrochemical behaviour of iron in alkaline solutions,Electrochim. Acta 23 (1978) 903-916.

[16] G.P. Kalaignan, V.S. Muralidharan, K.I. Vasu, Triangular potential sweep voltammetric study of porous iron electrodes in alkali solutions, J. Appl. Electrochem. 17 (1987) 1083-1092.